Aswan University Journal of Science and Technology Volume 4, issue 2, June 2024

ADAM optimization for adaptive position control of a cart driven by an armature-controlled DC motor supported by the Balloon effect

Mohamed Tarek [1,*], Salem Alkhalaf[2], Tomonobu Senjyu [3], Tarek Hassan, Ahmed Elnoby[1], and Ashraf Hemeida[1]

[1]Department of electrical engineering, Faculty of Energy Engineering, Aswan University, 81528 Aswan, Egypt
[2]Department of Information Technology, College of Computer, Qassim University, Buraydah, Saudi Arabia
[3]Department of Electrical and Electronics Engineering, Faculty of Engineering, University of the Ryukyus, Nishihara 903-0213, Japan;

Abstract

This research introduces a new method for controlling the linear positioning of a car powered by a DC motor with armature control, focusing on enhancing the parameters of the controller that is used to control the position of the car. The study employs the ADAM (Adaptive Moment Estimation) optimization algorithm and integrates the Balloon effect (BE) to improve the traditional ADAM algorithm's response, particularly against external disturbances and changes in system parameters. The proposed method includes an objective function dependent on the altered controller gain values and the determined value of the motor's open-loop transfer function. The system's performance with the proposed controller is evaluated under various conditions, including step load disturbances and variations in motor parameters. Both simulation and experimental results validate that the adaptive controller, utilizing the modified ADAM algorithm, significantly enhances the system's performance, particularly in mitigating load disturbances and uncertainties in system parameters.

Keywords: DC motor, ADAM optimization algorithm, Balloon Effect, Adaptive control

Introduction

DC motors are extensively utilized across diverse industries and applications because of their distinct qualities and adaptability. These motors play a crucial role in numerous devices and systems by transforming electrical energy into mechanical energy [1] [2]. The advantages of DC motors include Speed Control: DC motors offer excellent speed control capabilities. High Starting Torque: DC motors deliver high starting torque, enabling them to quickly accelerate heavy loads. Compact Size: DC motors are relatively compact and lightweight compared to other motor types Reversibility: DC motors can change their direction of rotation by simply reversing the polarity of the applied voltage.

In spite of their positive electrical and mechanical qualities, DC motors fall short of being perfect machines and come with certain drawbacks. These include Commutator and Brushes: These components can wear out over time, requiring regular maintenance and potentially causing issues such as sparking and brush noise Limited Speed Range: While DC motors offer excellent speed control, they have a limited speed range compared to some other motor types Complex Control Systems: Achieving precise speed and torque control in DC motors often requires complex control systems [3] [4]

*Corresponding author E-mail: moht1045@gmail.com
Received March 14, 2024 received in revised form, April 14, 2024, accepted April 19, 2024.
(ASWJST 2021/ printed ISSN: 2735-3087 and on-line ISSN: 2735-3095) https://journals.aswu.edu.eg/stjournal

their diverse range of applications DC motors are extensively utilized in fields like Electric vehicles: DC motors power electric cars, buses, and bicycles, offering efficient and reliable propulsion. Industrial machinery: DC motors drive conveyor systems, cranes, pumps, and various types of heavy machinery. Robotics: DC motors are used in robotic arms, grippers, and joints, providing precise and controlled movements, industrial automation, and renewable energy systems[5], [6]. They are commonly found in conveyor belts, pumps, fans, and compressors. Their high torque capability makes them suitable for driving heavy machinery and vehicles.

The PID controller is widely recognized and utilized in various industries due to its simplicity and effectiveness in enhancing both steady state and transient performance [7] PID has proven to be effective in various uses, one of which is its application in controlling DC motors [8],[9]. In practical operating conditions, controllers with fixed parameters that are designed according to typical operating conditions might not be applicable, thus requiring the implementation of online tuning techniques for PID (Proportional-Integral-Derivative) controllers.

Numerous examples of online tuning for PID controllers exist, providing valuable insights and references into this process. These examples encompass a range of techniques and methods aimed at achieving optimal control

Nomenclature

Symbol	Variable	Symbol	Variable
R	random value from 0 to 1	r_{mp}	motor pinion radius
J	Number of designed variables	K_g	planetary gearbox ratio
K	population size	T_{ai}	armature inertial torque
I	Number of iterations	J_m	rotor moment of inertia
$X(S)$	the position of the car	K_t	motor torque constant
$V_m(S)$	motor voltage	ζ_m	Efficiency of the motor
I_m	motor current	V_m	voltage motor
R_m	electric resistance of the motor	ADAM	Adaptive Moment Estimation
L_m	Inductance of the motor	BE	Balloon Effect
E_{emf}	back electromotive force voltage	Go(s)	Nominal transfer function
K_t	Motor torque constant		
M	The total mass of the car system		
F_{ai}	armature rotational inertial force		
F_C	Car driving force produced by the motor		
B_{eq}	equivalent viscous damping coefficient		
ζ_g	efficiency of gearbox		

performance for diverse systems. Here are a few prominent ones Zeigler-Nichols Method: A widely used approach for PID tuning involving step response analysis and relay feedback. It determines controller parameters based on the system's ultimate gain and oscillation period[10] atom search optimization (ASO): A controller tuning method focused on achieving specific performance criteria by considering process time constant and delay[11] Tyreus-Luyben Method: An extension of the Zeigler-Nichols Method that incorporates frequency response analysis. It improves performance by using the integral of the absolute error criterion (IAE) instead of the traditional squared error (ISE) [12] enhanced Bacterial Foraging Optimization (BFO) [13], [14], have been proposed to compute optimal parameters for the PID controller

Online tuning of PID parameters is possible, as shown in [15] which utilized genetic algorithms to successfully fine-tune PID parameters specifically for a continuous stirred tank reactor application. Additionally, neural networks have proved invaluable in addressing the adaptive control challenge for switched stochastic non-lower nonlinear triangular systems, as discussed in [16]. While these controllers have yielded favorable results, there is room for exploring and constructing novel algorithms to augment the effectiveness of adaptive controllers even further.

The ADAM algorithm, short for Adaptive Moment Estimation, is a popular and powerful optimization algorithm commonly used in the field of deep learning. It was first introduced by Diederik Kingma and Jimmy Ba in their 2015 ADAM combines the benefits of two other popular optimization algorithms, namely, Adaptive Gradient Algorithm (AdaGrad) and Root Mean Square Propagation (RMSProp). It aims to overcome their limitations while offering fast and efficient convergence during the training of neural networks [17]. It has been successfully applied in different domains, including Deep Learning: ADAM is widely employed in training deep neural networks. Its ability to handle large-scale datasets and intricate model architectures has made it a go-to optimization algorithm [18], Natural Language Processing: ADAM has been applied to various tasks in NLP, such as language modeling, machine translation, and sentiment analysis. Its robustness and good generalization capabilities make it a reliable choice in these domains [19], Computer Vision: ADAM finds extensive use in image classification, object detection, and image generation tasks [20], Recommender Systems: ADAM is employed for optimizing collaborative filtering and matrix factorization models in recommendation systems [21]

Furthermore, BE serves the objective of augmenting the prowess of optimization algorithms when it comes to delicately adjusting the parameters of a controller. This, in turn, amplifies its aptitude in effectively addressing challenges within a system, such as handling load disturbances and uncertainties associated with system parameters. The incorporation of this functionality is evident in the electro-search algorithm, which is deployed for adaptive load frequency control (as highlighted in [22]). Additionally, the water cycle algorithm (WCA) supported with BE for position control of a DC motor (as elaborated upon in [23]).

This study explores the application of a customized ADAM optimization technique to refine the gains of a position-velocity (PV) controller for an armature-controlled DC motor used in a car. Initially, the PV gains are determined using a conventional ADAM algorithm. However, in order to further enhance the performance of the system, the ADAM technique is customized by introducing a specific objective function (OF). The goal of this objective function is designed to minimize rise time, overshoot and settling time, thereby improving the overall system response. Although the classical ADAM method shows promising results, it may not always provide the optimal response in the presence of external disturbances or uncertainties in internal parameters. This limitation arises from the utilization of a predefined nominal system transfer function Go(S) when designing the objective function. To overcome this issue, the Balloon Effect (BE) is incorporated to augment the algorithm's sensitivity to system disturbances and uncertainties The manuscript provides the following contributions:

- The study proposes an adaptive position control method that utilizes ADAM optimization technique with support from BE.

- The suggested control method demonstrates efficient handling of system problems.

- As far as the authors are aware, this is the initial occurrence of ADAM and BE being employed in tandem as an adaptable position controller for a cart propelled by a DC motor.

2. Problem analysis

Different optimization techniques are utilized to address adaptive control challenges in various scenarios. These algorithms are commonly employed for parameter tuning of neural network or fuzzy controllers, as highlighted in references [24] and [25]. In such cases, the objective function is based on the error value of the controlled variable.

Furthermore, there have been efforts to directly apply optimization techniques for parameter tuning of adaptive controllers, as suggested in references [26] and [27]. However, these attempts use time response characteristics such as rise time, overshoot and settling time to build the objective function (e.g.,$J_{\min} = \sum(M_p + T_r + T_s)$. This approach has a drawback as M_p, T_s, and T_r are dependent on the nominal system parameter values, which poses challenges for time-variant systems.

A recent solution to address this issue is the introduction of a modification called the Balloon Effect (BE), described in references [22] and [23]. By integrating the BE modification, the objective function gains the ability to engage with recently updated parameter variations and other alterations in the system. In essence, the incorporation of the BE modification empowers straightforward optimization algorithms to efficiently fine-tune control parameters across a wide range of practical and industrial domains, spanning load frequency control, motor control and beyond

2. ADAM optimization algorithm (ADAM)

The Adam optimization algorithm is a highly efficient stochastic optimization method that achieves exceptional performance while utilizing only first-order gradients and conserving memory. It accomplishes this by dynamically calculating adaptive learning rates for each parameter, relying on estimations of the first and second moments of the gradients. The acronym "Adam" represents adaptive moment estimation, which amalgamates the strengths of two renowned techniques: AdaGrad, known for its efficiency with sparse gradients, and RMSProp. In our explanation, we establish clear connections between Adam and these and other stochastic optimization methods. One prominent advantage of Adam is its ability to maintain consistent magnitudes for parameter updates, regardless of gradient rescaling. Moreover, its step sizes are approximately bound by the step size hyperparameter. Unlike some methods, Adam does not necessitate a stationary objective, allowing it to adapt flexibly to evolving scenarios. Additionally, it adeptly handles sparse gradients and inherently introduces a form of step size annealing. [17].

2.1. Mathematical Representation:

ADAM maintains a set of adaptive learning rates for each parameter in the model. Let θ represent the parameters to be optimized, and $g_t$denotes the gradient of the objective function with respect to θ at time step t. The ADAM update rule can be represented as follows:

1. Initialize each of

- time step t = 0.
- the first moment vector (m) with zeros
- the second moment vector (v) with zeros
- the parameters to be optimized (θ).

2. While the stopping criterion is not met, do:

a. Increment the time step (t).

b. Compute the gradients (g) of the objective function with respect to the parameters.

c. Update the first moment estimates:

$$m_t = \beta_1 \, m_{(t-1)} + (1 - \beta_1) \, g_t \quad (1)$$

d. Update the second moment estimates:

$$v_t = \beta_2 \, v_{(t-1)} + (1 - \beta_2) \, {g_t}^2 \quad (2)$$

3. compensate for the bias of the initial moment estimates, ADAM applies bias correction:

$$\hat{m} = \frac{m_t}{1 - \beta^t_1} \quad (3)$$

$$\hat{v} = \frac{v_t}{1 - \beta^t_2} \quad (4)$$

where (t) is the current time step. These bias-corrected moment estimates are then used to update the parameters:

$$\theta = \theta - (\alpha \frac{\hat{m}}{\sqrt{v}+\varepsilon}) \quad (5)$$

In the above representation, α is the learning rate, β_1 and β_2 are hyperparameters controlling the exponential decay rates for the first and second moment estimates, respectively, ε is a small value added for numerical stability, g^2 represents element-wise squaring of the gradients

The ADAM optimization algorithm combines adaptive learning rates with momentum to efficiently optimize parameters in deep learning models. By maintaining adaptive moment estimates of the gradients, ADAM adapts the learning rate for each parameter individually, leading to faster convergence and better generalization performance. Its effectiveness and widespread adoption in various domains have made ADAM a popular choice in the deep learning community [18].

The following conventional ADAM algorithm notes are taken into consideration:

The traditional ADAM algorithm utilizes a matrix format to represent solutions. The size of the matrix is determined by multiplying the number of design variables by the population size. This expanded matrix enables the calculation of the highest and lowest solution values using the newly created solutions. To ensure stability during the initial stages of the system, it is recommended to initialize the values of the same design variable in proximity to each other. This practice mitigates excessive switching and instability issues. It's important to note that a larger population size and an increased number of iterations in the ADAM algorithm can lead to slower performance and compromise real-time characteristics. To address this, it is advisable to impose limitations on

the number of iterations that may not necessarily produce the best solution but still outperform the standard algorithm.

By preserving the optimal solution for future iterations, ADAM achieves improved and faster solutions. This strategy enhances the algorithm's capability to converge towards better solutions over time.

ADAM is a widely utilized algorithm in adaptive control, particularly for tuning different types of controllers like the PID controller tuning mentioned in Reference [28]. Fig. 1 illustrates an example implementation of ADAM for fine-tuning gains of the controller. In this scenario, the objective function of ADAM is formulated based on the closed-loop system's time response characteristics, including metrics like maximum overshoot (MP), rise time (Tr) and settling time (Ts). These evaluation parameters are influenced by the damping ratio (η) and natural frequency (ωn) which are in turn defined as functions within the initial open-loop transfer function Go(S). As depicted in Fig 1, during each iteration, $G_o(S)$ is determined according to two key concepts:

1) maintaining a disturbance equal to zero,
2) and using initial system parameters.

As a result, when using ADAM for adaptive control directly, the traditional ADAM method does not possess the capability to handle real-time variations in variable disturbances or system parameters. This deficiency represents a drawback in the conventional implementation of ADAM for adaptive control concerns.

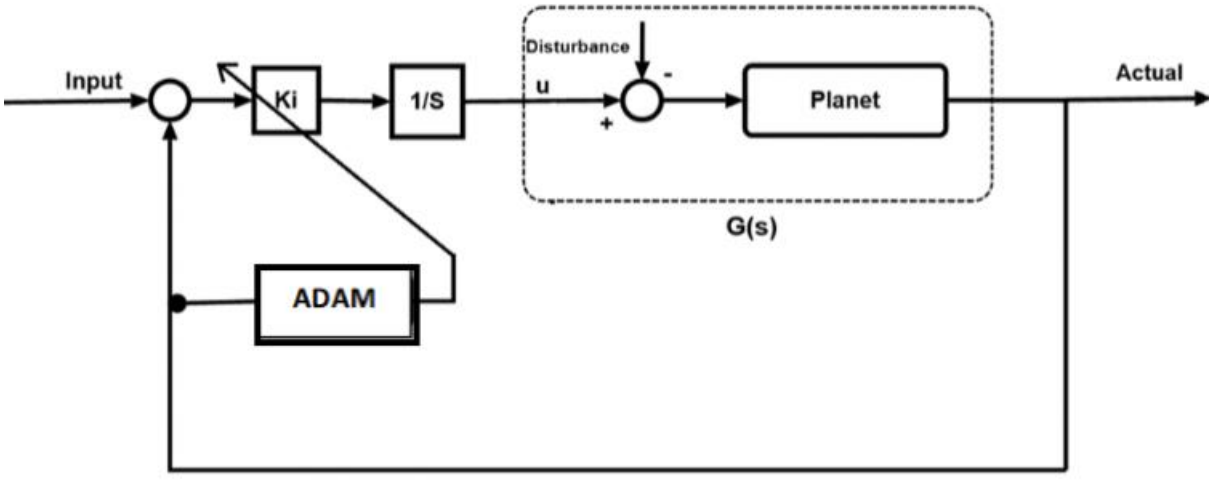

Fig. 1 traditional BOA system with open loop representation

2.2. ADAM with BE

To enhance the ADAM algorithm's capability in dealing with external disturbances or fluctuations in plant parameters, an additional component called BE has been introduced. The modified ADAM aims to improve its adaptability to external disturbances or variations in system parameters that may arise during any iteration. The concept of BE is illustrated in Fig. 3, while Fig. 2 showcases the depiction of the transfer function of system's open loop representation used in the modified ADAM algorithm at a specific iteration (i). The adjusted ADAM algorithm can be defined as follows:

1) At each iteration, the plant input $U_i$and plant output Y_i are used to feed the ADAM optimizer
2) $U_i$and Y_i may be used to determine the on-time transfer function.

$$G_i(S) = \frac{Y_i}{U_i} \quad (6)$$

3) The relation between $G_i(S)$ and $G_{i-1}(S)$

$$G_i(S) = AL_i \, {}^{*} G_{i-1}(S) \quad (7)$$

4)– Relation between $G_i(S)$ and $G_o(S)$ can be expressed as:

$$G_i(S) = AL_i \, {}^{*} G_{i-1}(S) \left(\prod_{n=1}^{i} AL_n\right) {}^{*} G_o(S) \quad (8)$$

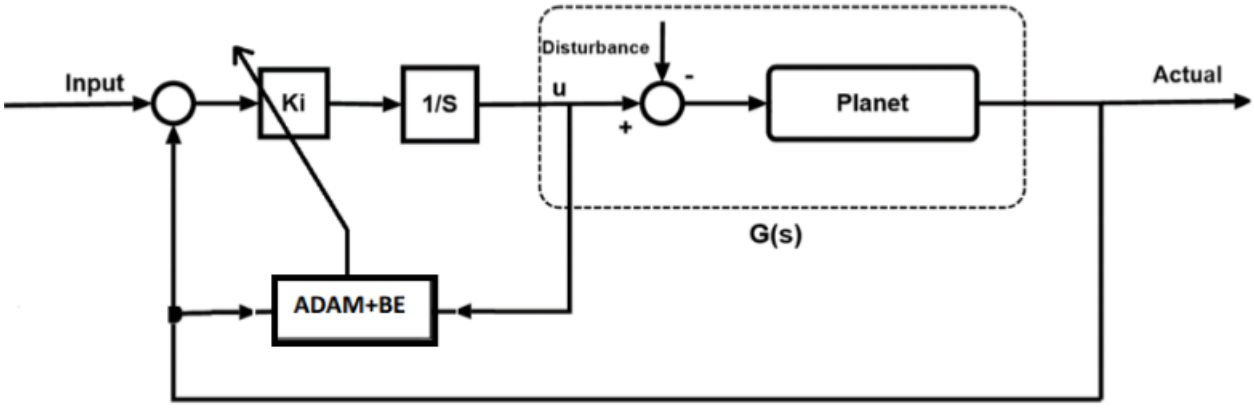

Fig. 2 System with considering open loop representation for ADAM with BE

The parameter AL_i signifies the influence of disturbances and variations in the parameters of the studded system during iteration (i). The shape of $G_i(S)$ is directly influenced by the value of AL_i, which is in turn affected by the uncertainties and disturbances present in the system. This phenomenon can be imagined as a balloon contracting or expanding in response to changes in air pressure, as illustrated in Fig. 3

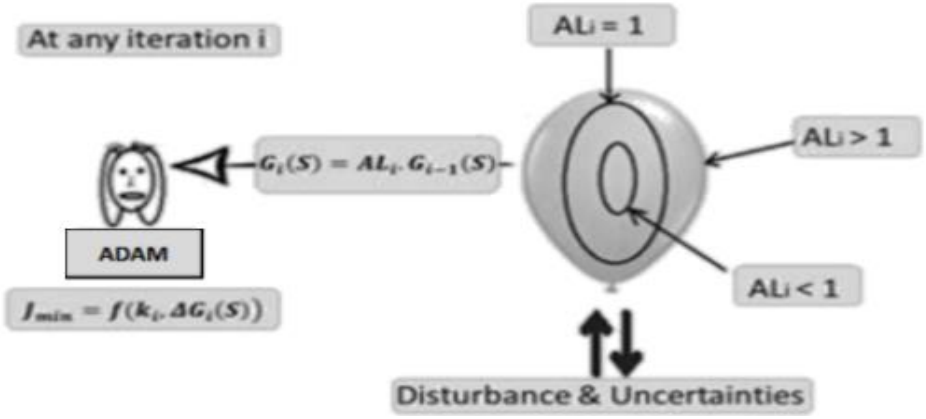

Fig. 3 Idea of ADAM with BE

Fig. 4 presents a flowchart outlining the utilization of ADAM with BE, an adaptive control technique suitable for a range of industrial applications including power system control and machine control. By referring to Eq. (8), the value of $G_i(S)$ is determined by both $G_o(S)$ and $(\prod_{n=1}^{i} AL_n)$, which encapsulates the impact of system issues. Consequently, the effectiveness of ADAM is influenced by the presence of system disturbances and uncertainties, leading to varied performance. In essence, the incorporation of BE in the control process enhances the sensitivity

of the objective function (OF) to system changes, thereby optimizing the efficiency of the control process facilitated by ADAM+BE for such scenarios.

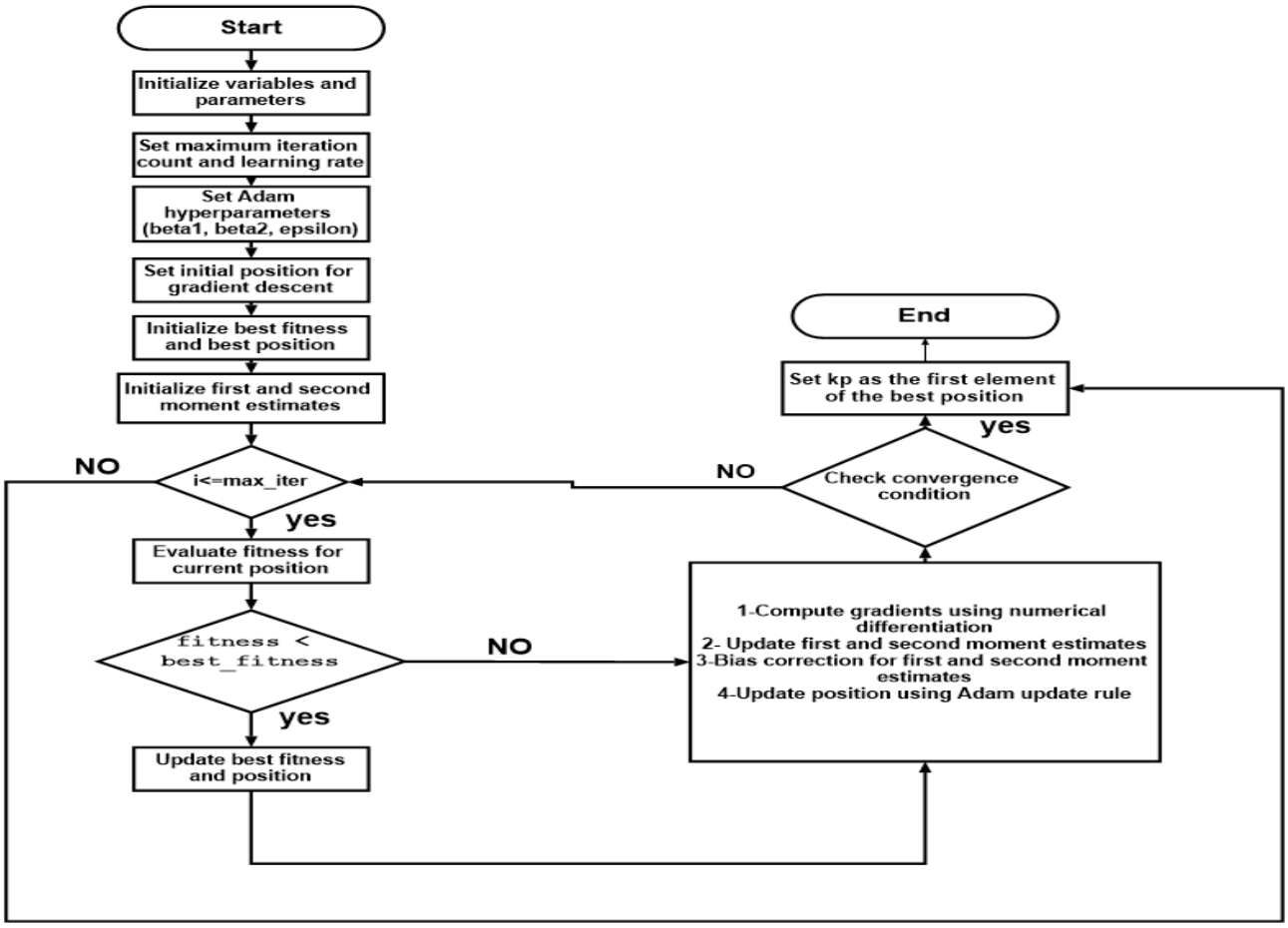

Fig. 4 Flowchart of Modified ADAM with BE

3. studded System

This manuscript zooms on a particular system illustrated in Fig. 5. It revolves around a cart maneuvered by an armature-controlled DC motor. The cart consists of an aluminum mass that glides along a shaft equipped with a linear bearing. The underlying movement is powered by a track-located DC motor, which is linked to a pinion mechanism aligned with a planetary gearbox [29].

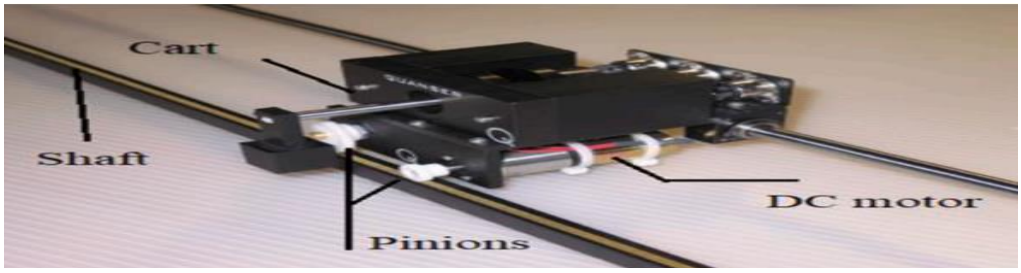

Fig. 5 Studied cart moved by DC motor

The car's system's behavior may be represented by an open loop transfer function, which is as follows:

$$G(S) = \frac{X(S)}{Vm(s)} \quad (9)$$

with reference to the Newton's second law:

$$M(\frac{d^2}{dt^2}x(t)) + F_{ai}(t) = F_c(t) - B_{eq}(\frac{d}{dt}x(t)) \quad (10)$$

to provide the armature inertial torque by:

$$F_{ai} = \frac{\eta_g K_g T_{ai}}{r_{mp}} \quad (11)$$

By utilizing Newton's second law, one can determine that:

$$J_m(\frac{d^2}{dt^2}\theta_m(t)) = T_{ai}(t) \quad (12)$$

The mechanical arrangement of the car's rack and pinion system can be calculated as:

$$\theta_m = \frac{K_g X}{r_{mp}} \quad (13)$$

The motor's driving force F_c can be calculated using:

$$F_c = \frac{\eta_g K_g T_m}{r_{mp}} \quad (14)$$

The DC motor's torque can be stated as follows:

$$`T_m = \eta_m K_t I_m \quad (15)$$

Furthermore, the angular velocity of the motor may be written as:

$$\omega_m = \frac{K_g(\frac{d}{dt}X(t))}{r_{mp}} \quad (16)$$

Fig .6 depicts the armature circuit of a typical DC motor. This electrical circuit's use of Kirchhoff's voltage law is illustrated as:

$$V_m - R_m I_m - L_m(\frac{d}{dt}I_m) - E_{emf} = 0 \quad (17)$$

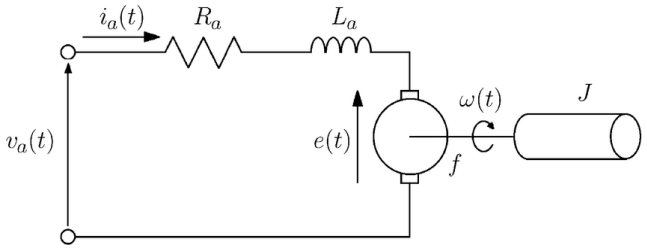

Fig.6 the DC motor's armature circuit

By ignoring the motor's inductance, we get I_{m}

Table 1 studded Values of system parameters

Symbol	value	Symbol	value
ζ_g	100%	r_{mp}	$6.35*10^{-3}$ M
ζ_m	100%	K_g	3.71
K_t	$7.67*10^{-3}$ N.m/A	R_m	2.6 ohm
M	0.97 Kg	J_m	$3.9*10^{-7}$ Kg. m^2

$$I_m = \frac{V_m - E_{emf}}{R_m \; r_{mp}} \tag{18}$$

Finally, the motor's (TF) can be determined as:

$$G(S) = \frac{r_{mp}\eta_g K_g \eta_m K_t}{(R_m M r_{mp}^2 + R_m \eta_g K_g^2 J_m)S^2 + (\eta_g K_g^2 \eta_m K_t K_m + B_{eq} R_m r_{mp}^2)S} \tag{19}$$

Fig. presents the block diagram, providing comprehensive information about the under-study armature-controlled DC motor. Detailed data regarding the system components can be found in

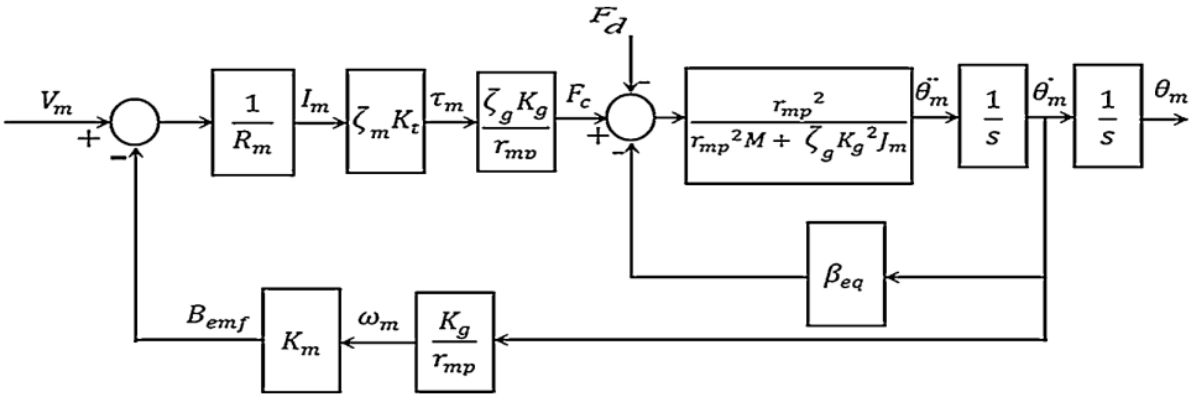

[29]. Additionally, Fig. **7** Block diagram showing how the employed DC motor is designed

Table 2 displays the maximum values associated with the electrical motor.

Symbol	value	Symbol	value
V	6 V	I	1 A
F	50 HZ	Ω	628.3 rad/sec

Fig. 7 Block diagram showing how the employed DC motor is designed

Table 2 Maximum electrical motor parameter values

4. adaptive control of the studded system using ADAM algorithm

In Fig. 8, we can observe the structure of the PV controller, and $G(S)$ represents a schematic of the studded DC motor. The parameters K_{p0} (the initial value of K_p) and K_{v0} (the initial value of K_v) can be denoted as:

K_{v0} = 5.532 V.sec/m and K_{p0} = 274.62 V/m. These specific values have been chosen to achieve system parameters including 0.15 seconds rise time and a 10% overshoot. The objective of ADAM optimization is to precisely adjust the gains K_p and K_v of the PV controller.

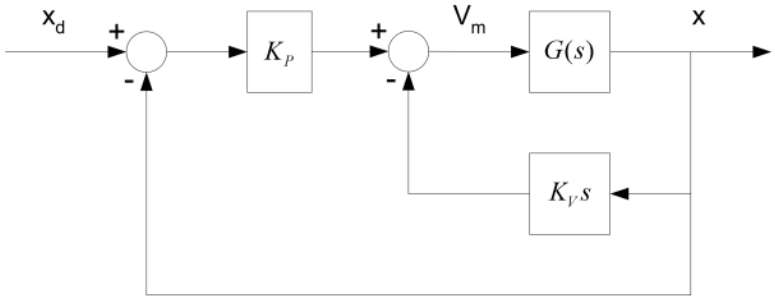

Fig. 8 structure of the PV controller

4.1. Traditional ADAM for optimizing PV controller

Fig. depicts a position controller for the studded motor utilizing the traditional ADAM optimization method. In order to optimize ADAM's objective function, it is necessary to determine the closed-loop transfer function of the system using Equation (19) while taking into account the nominal data provided in

. Subsequently, further steps can be undertaken:

$$G_o(S) = \frac{2.46}{s^2+17.13s} \quad (18)$$

Symbol	value	Symbol	value
V	6 V	I	1 A
F	50 HZ	Ω	628.3 rad/sec

And the feedback transfer function may be expressed as follows, as seen in Fig .9:

$$\frac{X_i}{X_{di}} = \frac{2.46^*K_{pi}}{S^2+(17.13+2.46^*K_{vi})S+(2.46^*K_{pi})} \quad (19)$$

Considering Eq. (21), it is worth mentioning that $\omega_{ni}, \eta_i, T_{ri}, T_{si}, M_{pi}$ and $J_{\min}$ will solely depend on the newly updated values of PV controller gains K_{pi} and K_{vi} throughout all iterations.

4.2. ADAM with BE for optimizing PV controller

In Fig .9, you can observe the implementation of the adaptive position control system using the innovative ADAM algorithm that incorporates BE. During each iteration, the closed-loop transfer function value of the system can be computed by utilizing equations (8) and (19), while referring to the configuration depicted in Fig .9. The computation process is as outlined below:

$$\frac{X_i}{X_{di}} = \frac{2.46^*(\prod_{n=1}^{i} AL_n)*K_{pi}}{S^2+(17.13+2.46^*K_{vi}{}^*(\prod_{n=1}^{i} AL_n))S+(2.46^*K_{pi}{}^*(\prod_{n=1}^{i} AL_n))} \quad (20)$$

Where

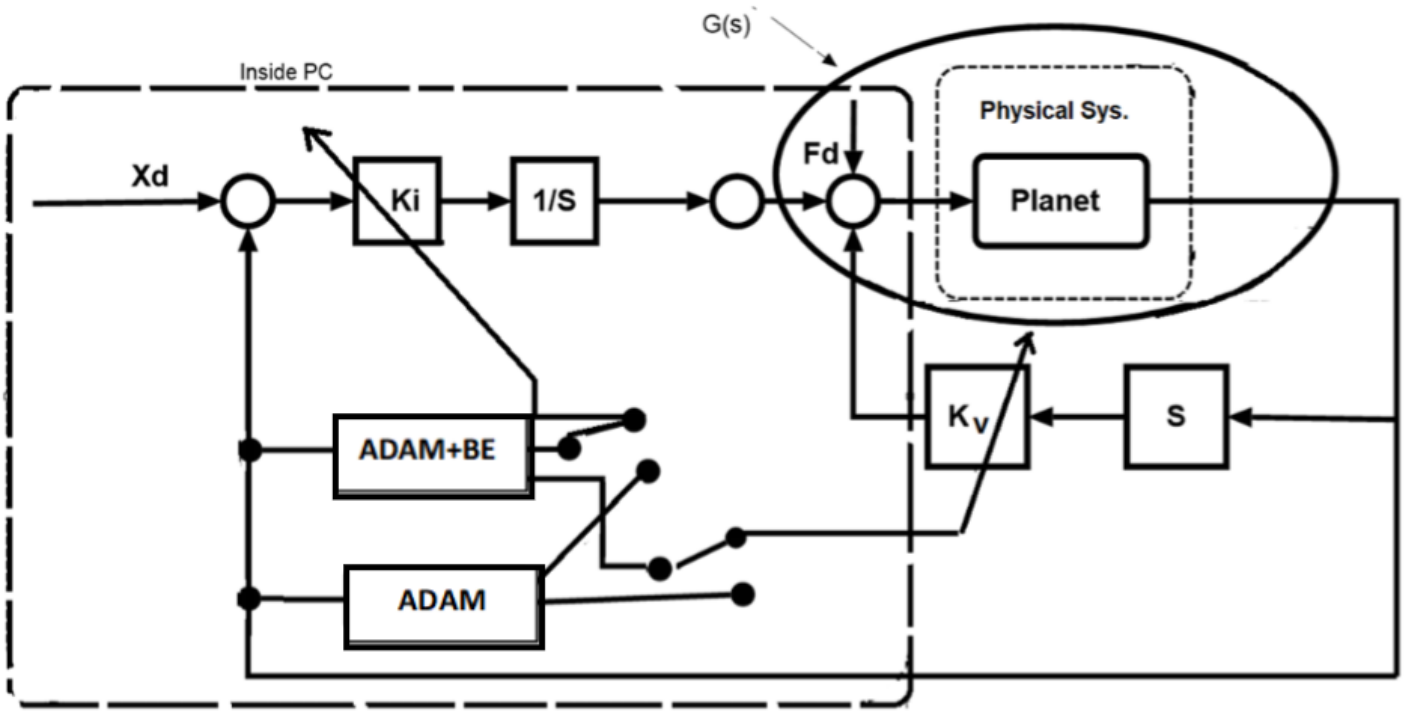

$$\omega_{ni} = \sqrt{2.46 * (\prod_{n=1}^{i} AL_n) K_{pi}}$$

Fig. 9 Block schematic of the controller-equipped system

And

$$\eta_i = \frac{(17.13 + 2.46 * K_{vi}^*(\prod_{n=1}^{i} AL_n))}{2 * \omega_{ni}}$$

The parameters M_{pi}, T_{ri} and T_{si} for the second-order closed-loop system are calculated using the values ω_{ni} and η_i. The minimum objective function, $J_{\min}$, in ADAM+BE is influenced by K_{pi}, K_{vi}, and the term $\left(\prod_{n=1}^{l} AL_n\right)$, which represents system disturbances and parameter variations.

The correlation between the problem and the algorithm can be understood as stated below: In each iteration, the ADAM algorithm with BE receives input $U_i$and the output X_i from the plant. These signals are used to calculate $G_i(S)$ using Equation (2), while the previously stored value of $G_{i-1}(s)$ is used to determine AL_i. This value, along with its accumulated historical values, is used to calculate $\left(\prod_{n=1}^{l} AL_n\right)$. At the same time, within the ADAM algorithm loops, candidate values of K_pi and K_vi are computed. These values are then combined with $\left(\prod_{n=1}^{l} AL_n\right)$to determine the parameters M_{pi}, T_{ri} and T_{si} for the time response.

These parameters are used to evaluate the value of the objective function, $J_{\min}$ which ultimately determines the optimal and final values of $K_{pi}$and K_{vi}. These values are then passed to the Simulink program as part of the PV controller. The Simulink program generates control signals that are sent to the physical process via a Data Acquisition card.

The effectiveness of the proposed control scheme relies on the specifications of the computer used, including factors such as the speed of the processor, cache memory, and RAM capacity.

Simulation results

Table 3 provides a list of the parameters for the ADAM algorithm. The selected objective function for this

beta1	ADAM hyperparameter
beta2	ADAM hyperparameter
m_ K_p & m_ K_v	First moment estimate for both $K_p$and K_v.
v_ K_p & v_ K_v	Second moment estimate for both $K_p$and K_v
Initial_ position	Initial position for gradient descent

implementation is:

$$J_{\min} = \sum(M_p^2 + T_r^2 + T_s^2)$$

The proposed control algorithm for the DC motor system was implemented using the Simulink package in MATLAB, which served as the simulation environment

Table 3 Selected parameters of ADAM

In this research, the physical disruption was substituted with a comparable voltage for the purpose of measuring. The method of combining point movement, shown in Fig 10, was employed to accomplish this. The system being studied underwent testing for both sudden changes in the desired input and sudden load disturbances. To evaluate the influence on the suggested system, an equivalent load disturbance, illustrated in Fig 11, was introduced. It commenced at t=3 seconds and concluded at t=5 seconds, with a value of 0.95 volts. The signal for the desired motor position began at 1.5 seconds, with an initial displacement of 15 mm, and ended at 6 seconds

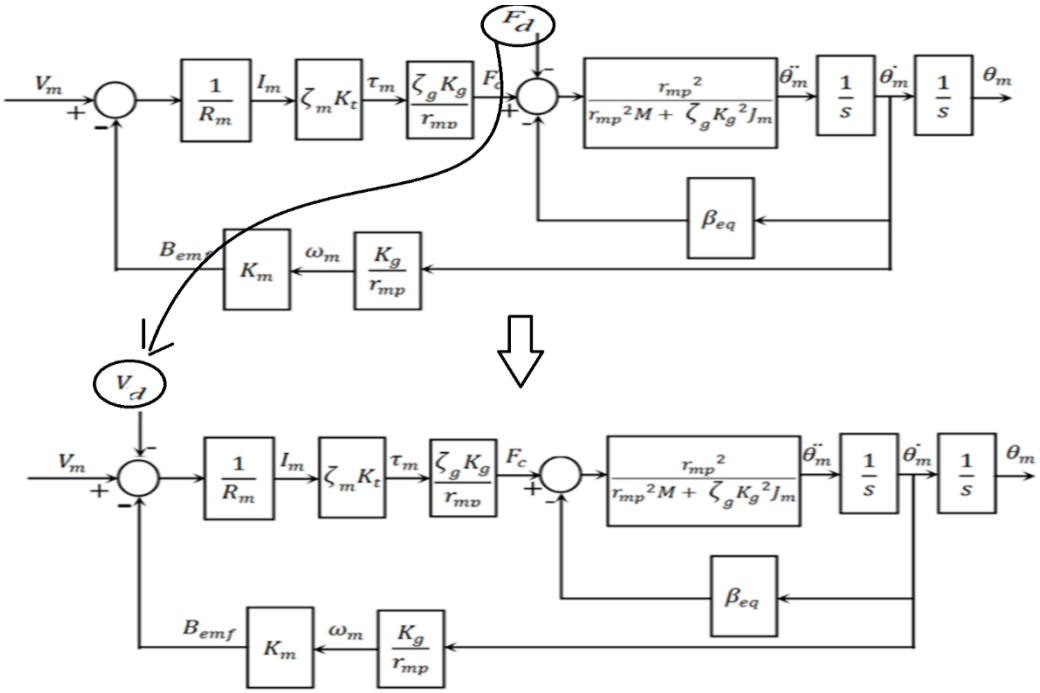

Fig. 10. The option of sum point movement

The performance of two different systems was compared: one with a controller tuned using the classical ADAM algorithm, and the other with a traditional PV controller. Based on the results shown in Fig 12, it was observed that using the PV controller tuned by the normal ADAM algorithm reduced overshoot by approximately 30% compared to the fixed parameters PV controller. Another comparison was made between systems utilizing the classical ADAM algorithm and the modified ADAM algorithm with BE during load disturbance and step reference change, with corresponding results shown in Fig 13 and Fig 14.

Fig 13 demonstrates that the proposed ADAM algorithm with BE achieved a rise time of around 0.06 seconds, while the normal ADAM algorithm resulted in a rise time of approximately 0.2 seconds. The adaptive PV controller, tuned by the proposed ADAM algorithm with BE, also exhibited improved overshoot during step disturbance. Detailed parameters can be found in Table 4.

Table 4 highlights that the proposed ADAM algorithm with BE yielded the best values for overshoot, rise time, and settling time compared to the conventional PV controller. However, when comparing the system with the classical ADAM algorithm, it was found to have better overshoot but similar rise time and settling time. Both Fig 12 and Fig 14 demonstrate that the suggested adaptive PV controller, tuned by either the normal ADAM algorithm or the

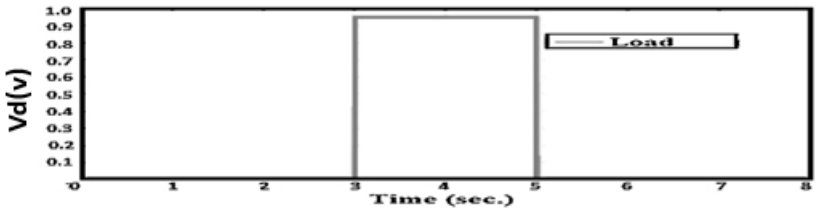

Fig. 11 Load disturbance

modified ADAM algorithm with BE, effectively addressed the issue of load disturbance. Furthermore, the performance of the modified ADAM technique surpassed other.

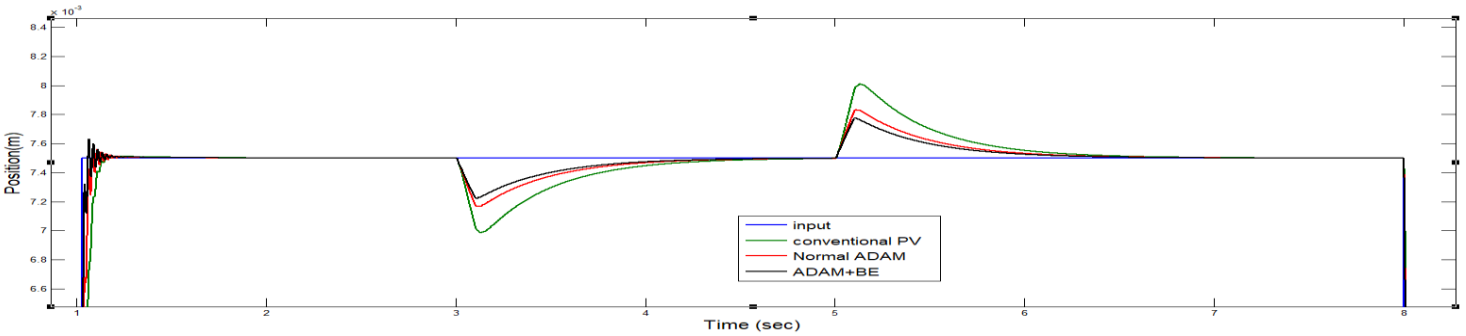

Fig.12 the outcome of tunning PV controller using conventional BOA in the event of a load disturbance

The performance of the proposed ADAM algorithm with BE outperforms the normal ADAM algorithm, as demonstrated in Fig. 14. This figure illustrates the tuned values of K_p and K_v using both the normal ADAM

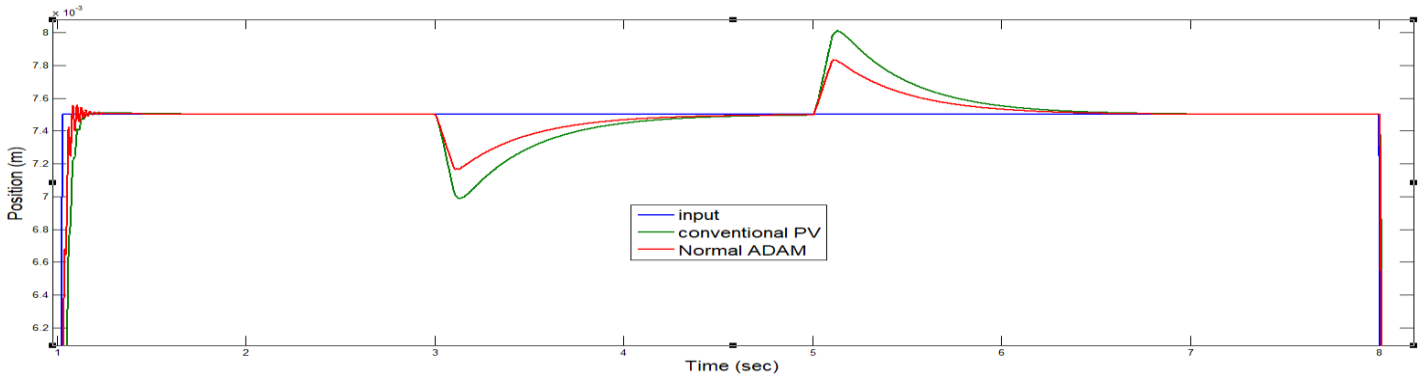

Fig. 13 the outcome of tunning PV controller using conventional ADAM/ADAM+BE in the event of a load disturbance.

algorithm and the proposed ADAM algorithm with BE. It visually represents the significant effort made by the proposed scheme to adjust K_p and K_v in order to effectively address system problems.

Table 4 Time response parameters

	M_p	T_r(sec)	T_s(sec)
Conventional PV	2.3%	0.2	0.4
Normal BOA	1.1%	0.2	0.4

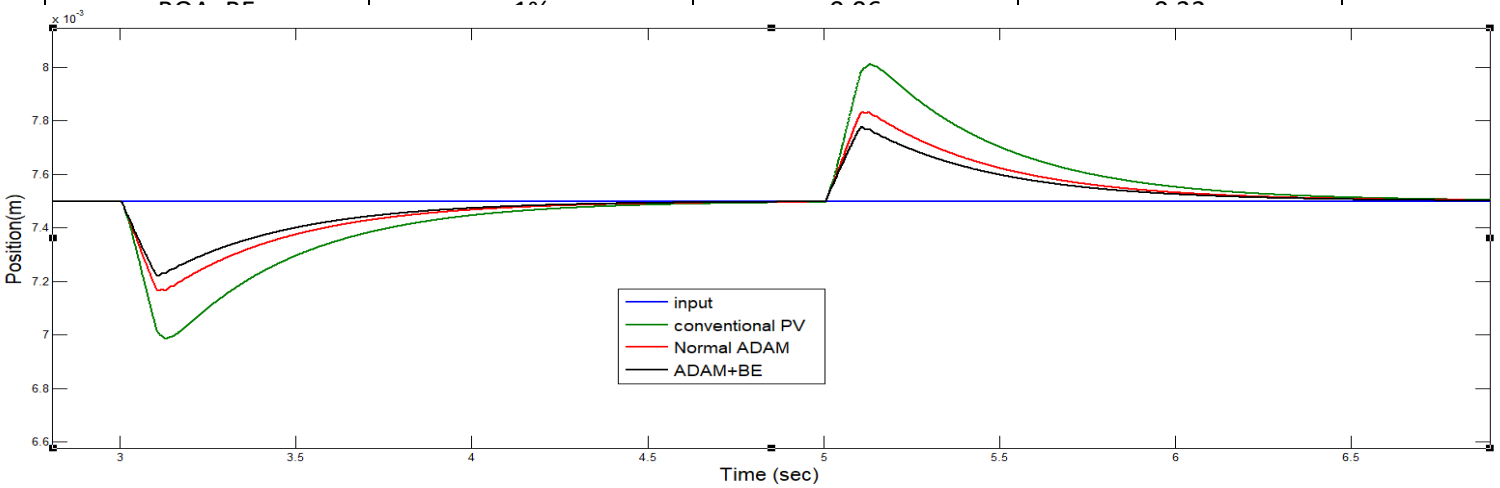

Fig. 14 the outcome of tunning PV controller using conventional ADAM/ADAM+BE in the event of a load disturbance

Experimental results

Fig. 15 shows the actual implementation of the proposed car, which is driven by a DC motor. The communication between MATLAB running on a PC and the DC motor was facilitated through the QPIDe data acquisition card and the QuanserVoltPAQ voltage amplifier unit. To determine the position, a single-ended optical shaft encoder was utilized as a sensor [29]. The hardware setup is depicted in Fig. 16.

The experimental setup replicated the same test cases used in the simulation. The results obtained from the experiments are presented in Fig .17, Fig .18, and Fig .19. Fig .17 illustrates the system responses for both the classical and tuned PV controllers. It is evident that the suggested adaptive technique had a positive impact on the system's response to step load changes and step inputs. Using the normal ADAM algorithm, the overshoot was reduced by approximately 35% compared to the conventional PV controller.

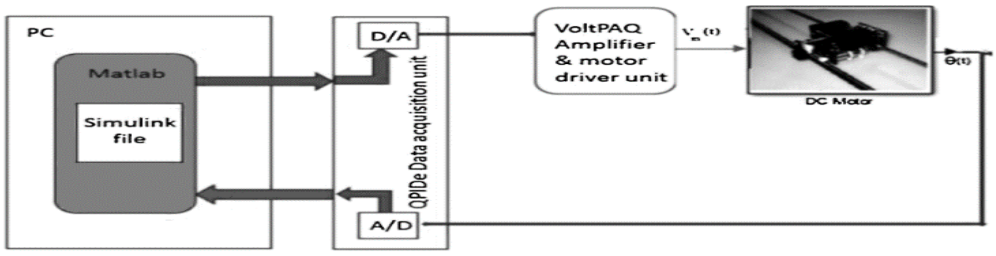

Fig. 15 The proposed system using digital MATLAB controller

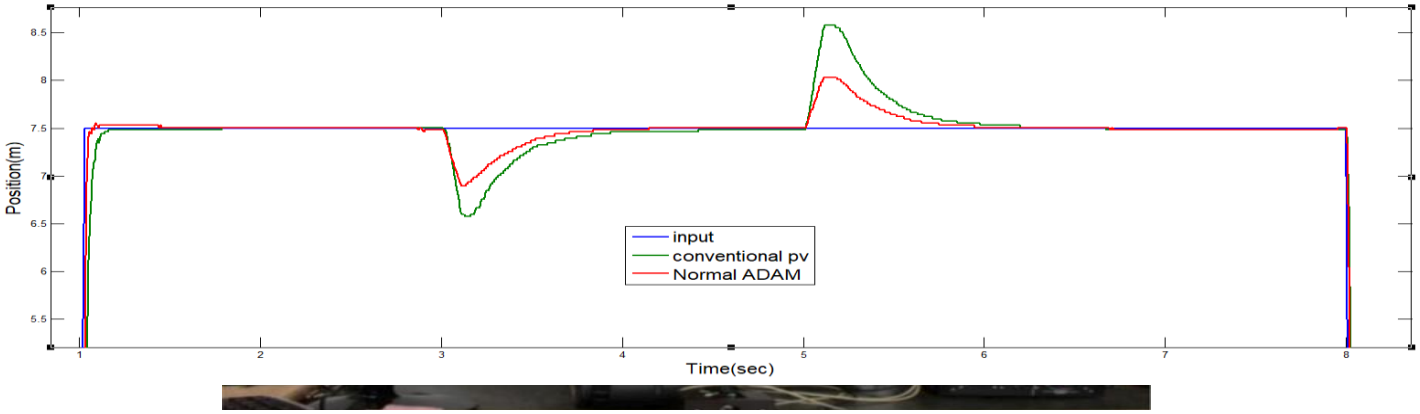

Fig. 17 The result of the system with conventional /adaptive PV controller

Fig. 16 Experimental setup

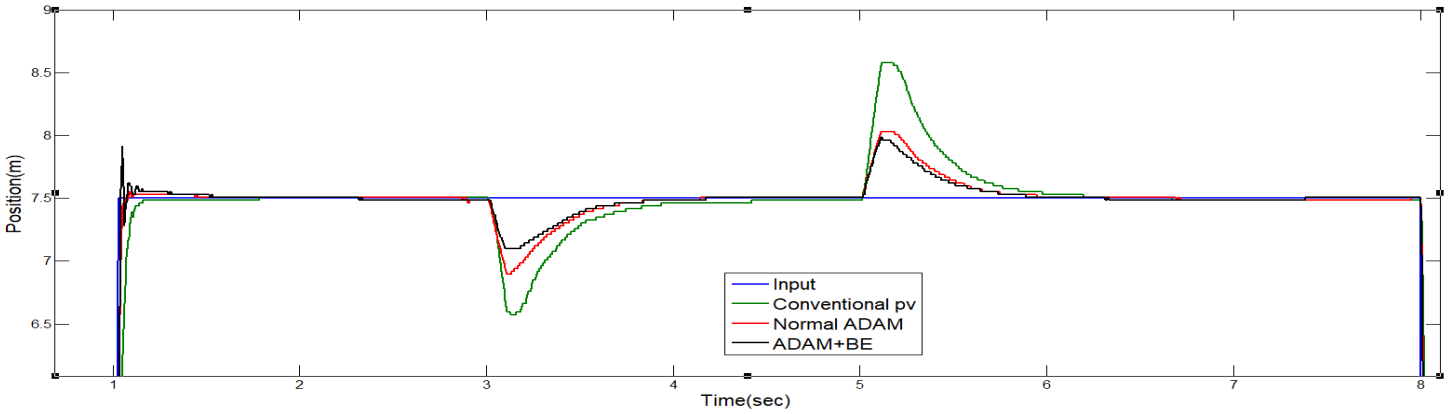

Fig. 18 The result of adaptive PV controller with normal / modified ADAM, In case of load disturbance

Furthermore, Fig .18 highlights the superiority of the system with the modified ADAM algorithm with BE over the system with the normal ADAM algorithm when subjected to load disturbance. It is evident that the system response using the modified ADAM algorithm with BE is smooth and stable, while the system response using the normal ADAM algorithm exhibits poor performance during the initial three seconds, accompanied by high ripples.

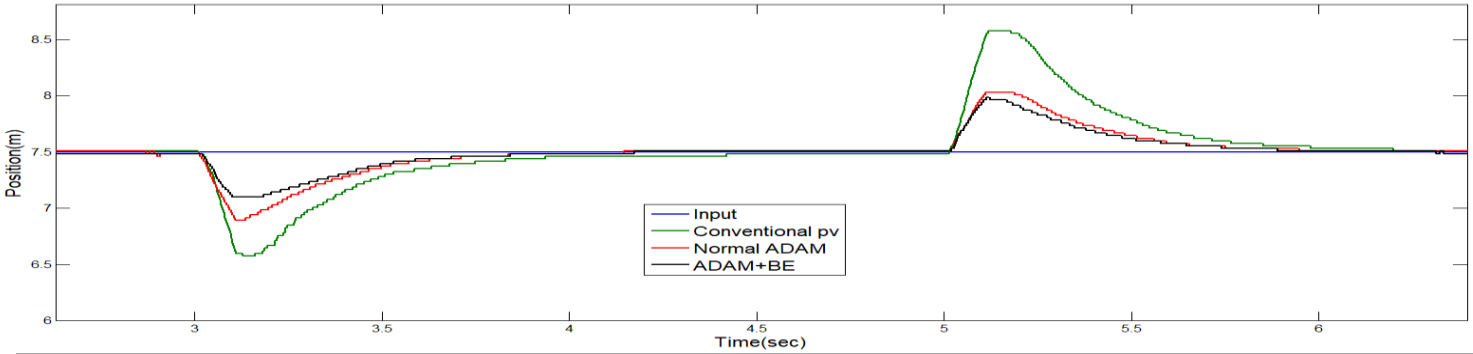

Based on the experimental findings, it is evident that the system utilizing the PV controller tuned by the proposed ADAM algorithm with BE exhibits greater resilience compared to the system employing the controller tuned by the traditional ADAM technique. To further scrutinize and compare the optimization between ADAM and ADAM with BE, specific time instances (t = 3 sec. and t = 5.5 sec.) were selected for the optimization evaluation. The comparison data was recorded and displayed using program code, as shown in Table 5.

The data presented in Table 5 serves as evidence that the adaptive controller tuned by ADAM with BE demonstrates superior performance in terms of M_p (maximum overshoot), T_r (rise time), T_s (settling time), and ISE (integral square error) during critical moments such as the onset and cessation of step load disturbances, in contrast to the system with the adaptive controller tuned by the classical ADAM algorithm.

Table 5 An optimization comparison between ADAM and ADAM + BE

	ADAM						**ADAM+BE**					
T(sec)	K_{pi}	K_{vi}	$\|M_{pi}\|$	T_{ri}	T_{si}	ISE	K_{pi}	K_{vi}	$\|M_{pi}\|$	T_{ri}	T_{si}	ISE
3	909	41	1.6%	0.23	0.503	1.2	774	27	1.03%	0.02	0.4	0.51
5.5	737	44	1.4%	0.16	0.42	0.60	599	32	0.96%	0.91	0.040	0.32

Conclusions

In summary, this research paper introduces an adaptive control technique that employs the ADAM optimization algorithm enhanced by BE. The main objective was to utilize this control method to adjust the gains of the PV controller, enabling precise control over the linear position of a cart propelled by a DC motor. By incorporating BE into the ADAM algorithm, the control technique underwent significant enhancement, enhancing its ability to handle load disturbances and uncertainties in system parameters. Moreover, the integration of BE in the ADAM algorithm resulted in overall improvement in essential system characteristics, including overshoot, settling time, and rise time. To evaluate the performance of the proposed adaptive controller using ADAM with BE, rigorous testing during external step disturbances was conducted, revealing exceptional and noteworthy outcomes. A comprehensive comparison was also carried out between the system employing the modified ADAM algorithm and the system utilizing the conventional ADAM algorithm, taking into account external disturbances and changes in system parameters. Consistently, both simulation and experimental results affirmed the superiority of the system with the proposed ADAM with BE across all examined scenarios with the presence of some limitations like Complexity, Implementing the ADAM algorithm with the Balloon effect may increase the complexity of the controller tuning process, requiring a deeper understanding of both algorithms and their interactions and Sensitivity to Hyperparameters, The performance of the ADAM algorithm and the Balloon effect can be sensitive to their respective hyperparameters, requiring careful tuning to achieve optimal results.

References

1] J Chapman, Stephen. *Electric machinery fundamentals*. McGraw-hill, 2004.forth edition

2] Fitzgerald, A. E., Kingsley, C., Umans, S. D., & Wildi, T. (2016). Electric machinery. McGraw-Hill Education

3] Premkumar, K., and B. V. Manikandan. "Adaptive Neuro-Fuzzy Inference System based speed controller for brushless DC motor." *Neurocomputing* 138 (2014): 260-270. https://doi.org/10.1016/j.neucom.2014.01.038

4] Abro, Kashif Ali, J. F. Gómez-Aguilar, Ilyas Khan, and K. S. Nisar. "Role of modern fractional derivatives in an armature-controlled DC servomotor." *The European Physical Journal Plus* 134, no. 11 (2019): 553. https://doi.org/10.1140/epjp/i2019-12957-6

5] Neethu, U., and V. R. Jisha. "Speed control of Brushless DC Motor: A comparative study." In *2012 IEEE international conference on power electronics, drives and energy systems (PEDES)*, pp. 1-5. IEEE, 2012. https://doi.org/10.1109/PEDES.2012.6484349

6] Bhatt, Pooja, Hemant Mehar, and Manish Sahajwani. "Electrical motors for electric vehicle–a comparative study." *Proceedings of Recent Advances in Interdisciplinary Trends in Engineering & Applications (RAITEA)* (2019). https://dx.doi.org/10.2139/ssrn.3364887

7] R. Saidur, "A review on electrical motors energy use and energy savings," *Renewable and Sustainable Energy Reviews*, vol. 14, no. 3. pp. 877–898, Apr. 2010. doi: 10.1016/j.rser.2009.10.018.

8] H. S. Purnama, T. Sutikno, S. Alavandar, and A. C. Subrata, "Intelligent Control Strategies for Tuning PID of Speed Control of DC Motor - A Review," in *CENCON 2019 - 2019 IEEE Conference on Energy Conversion*, Institute of Electrical and Electronics Engineers Inc., Oct. 2019, pp. 24–30. doi: 10.1109/CENCON47160.2019.8974782.

9] H. S. Purnama, T. Sutikno, S. Alavandar, and A. C. Subrata, "Intelligent Control Strategies for Tuning PID of Speed Control of DC Motor - A Review," in *CENCON 2019 - 2019 IEEE Conference on Energy Conversion*, Institute of Electrical and Electronics Engineers Inc., Oct. 2019, pp. 24–30. doi: 10.1109/CENCON47160.2019.8974782.

10] Ziegler, John G., and Nathaniel B. Nichols. "Optimum settings for automatic controllers." *Transactions of the American society of mechanical engineers* 64, no. 8 (1942): 759-765. https://doi.org/10.1115/1.4019264

11] C. I. Muresan, S. Folea, G. Mois, and E. H. Dulf, 'Development and implementation of an FPGA based fractional order controller for a DC motor', *Mechatronics*, vol. 23, no. 7, pp. 798–804, 2013, doi: 10.1016/j.mechatronics.2013.04.001.

12] Wang, L., and W. R. Cluett. "Tuning PID controllers for integrating processes." *IEE Proceedings-Control Theory and Applications* 144.5 (1997): 385-392. https://doi.org/10.1049/ip-cta:19971435

13] Latha, K., and V. Rajinikanth. "2DOF PID controller tuning for unstable systems using bacterial foraging algorithm." *Swarm, Evolutionary, and Memetic Computing: Third International Conference, SEMCCO 2012, Bhubaneswar, India, December 20-22, 2012. Proceedings 3*. Springer Berlin Heidelberg, 2012. https://doi.org/10.1007/978-3-642-35380-2_61

14] V. Rajinikanth and K. Latha, "Controller Parameter Optimization for Nonlinear Systems Using Enhanced Bacteria Foraging Algorithm," *Applied Computational Intelligence and Soft Computing*, vol. 2012, pp. 1–12, 2012, doi: 10.1155/2012/214264.

15] A. Jayachitra and R. Vinodha, "Genetic Algorithm Based PID Controller Tuning Approach for Continuous Stirred Tank Reactor," *Advances in Artificial Intelligence*, vol. 2014, pp. 1–8, Dec. 2014, doi: 10.1155/2014/791230.

16] B. Niu, P. Duan, J. Li, and X. Li, "Adaptive Neural Tracking Control Scheme of Switched Stochastic Nonlinear Pure-Feedback Nonlower Triangular Systems," *IEEE Trans Syst Man Cybern Syst*, vol. 51, no. 2, pp. 975–986, Feb. 2021, doi: 10.1109/TSMC.2019.2894745.

17] Kingma, Diederik P., and Jimmy Ba. "Adam: A method for stochastic optimization." arXiv preprint arXiv:1412.6980 (2014). https://doi.org/10.48550/arXiv.1412.6980

18] Zhang, Zijun. "Improved adam optimizer for deep neural networks." In *2018 IEEE/ACM 26th international symposium on quality of service (IWQoS)*, pp. 1-2. Ieee, 2018. https://doi.org/10.1109/IWQoS.2018.8624183

19] Xie, Sang, Jian Liu, Jianming Xiao, and Xiugui Liu. "Rational homotopy types of mapping spaces via cohomology algebras." *Archiv der Mathematik* 119, no. 6 (2022): 639-648. https://doi.org/10.1007/s00013-022-01784-4

20] Lu, Yongxi, Tara Javidi, and Svetlana Lazebnik. "Adaptive object detection using adjacency and zoom prediction." In *Proceedings of the IEEE conference on computer vision and pattern recognition*, pp. 2351-2359. 2016.

21] De Boom, Cedric, Rohan Agrawal, Samantha Hansen, Esh Kumar, Romain Yon, Ching-Wei Chen, Thomas Demeester, and Bart Dhoedt. "Large-scale user modeling with recurrent neural networks for music discovery on multiple time scales." *Multimedia Tools and Applications* 77 (2018): 15385-15407. https://doi.org/10.1007/s11042-017-5121-z

22] Y. A. Dahab, H. Abubakr, and T. H. Mohamed, "Adaptive load frequency control of power systems using electro-search optimization supported by the balloon effect," *IEEE Access*, vol. 8, pp. 7408–7422, 2020, doi: 10.1109/ACCESS.2020.2964104.

23] T. H. Mohamed, H. Abubakr, M. A. M. Alamin, and A. M. Hassan, "Modified WCA-Based Adaptive Control Approach Using Balloon Effect: Electrical Systems Applications," *IEEE Access*, vol. 8, pp. 60877–60889, 2020, doi: 10.1109/ACCESS.2020.2982510.

24] V. Rajinikanth and K. Latha, "Setpoint weighted PID controller tuning for unstable system using heuristic algorithm," *Archives of Control Sciences*, vol. 22, no. 4, pp. 481–505, 2012, doi: 10.2478/v10170-011-0037-8.

25] M. H. Khooban, T. Niknam, F. Blaabjerg, P. Davari, and T. Dragicevic, "A robust adaptive load frequency control for micro-grids," *ISA Trans*, vol. 65, pp. 220–229, Nov. 2016, doi: 10.1016/j.isatra.2016.07.002

26] W. I. Gabr *et al.*, *2018 Twentieth International Middle East Power Systems Conference (MEPCON) : conference proceedings : Cairo University, Cairo, Egypt, December 18-20, 2018 (MEPCON'2018).* https://doi.org/10.1109/MEPCON.2018.8635216

27] Mohamed, Tarek, Hussein Abubakr, Mahmoud M. Hussein, and Gaber Shabib. "Load frequency controller based on particle swarm optimization for isolated microgird system." *International Journal of Applied Energy Systems* 1, no. 2 (2019): 69-75. https://doi.org/10.21608/ijaes.2019.169953

28] Dai, Mingjun, Zelong Zhang, Xiong Lai, Xiaohui Lin, and Hui Wang. "PID controller-based adaptive gradient optimizer for deep neural networks." *IET Control Theory & Applications* 17, no. 15 (2023): 2032-2037. https://doi.org/10.1049/cth2.12404

29] Quanser, " Linear experiment #1: PV position control, " Internet: http://www.ece.uprm.edu/control/manual/quanser/linear/IP01_2%20Position_PV_Student_ 504.pdf, [April. 5, 2020].

30] Mohamed, Tarek Hassan, Mohamed Abdelhamid Mohamed Alamin, and Ammar M. Hassan. "Adaptive position control of a cart moved by a DC motor using integral controller tuned by Jaya optimization with Balloon effect." *Computers & Electrical Engineering* 87 (2020): 106786. https://doi.org/10.1016/j.compeleceng.2020.106786

31] Mohamed, Tarek Hassan, Mohamed Abdelhamid Mohamed Alamin, and Ammar M. Hassan. "A novel adaptive load frequency control in single and interconnected power systems." *Ain Shams Engineering Journal* 12, no. 2 (2021): 1763-1773. https://doi.org/10.1016/j.asej.2020.08.024